

# Hartree-Fock treatment of Fermi polarons using the Lee-Low-Pine transformation

Ben Kain<sup>1</sup> and Hong Y. Ling<sup>2</sup>

<sup>1</sup>*Department of Physics, College of the Holy Cross, Worcester, Massachusetts 01610 USA*

<sup>2</sup>*Department of Physics and Astronomy, Rowan University, Glassboro, New Jersey 08028 USA*

We consider the Fermi polaron problem at zero temperature, where a single impurity interacts with non-interacting host fermions. We approach the problem starting with a Fröhlich-like Hamiltonian where the impurity is described with canonical position and momentum operators. We apply the Lee-Low-Pine (LLP) transformation to change the fermionic Fröhlich Hamiltonian into the fermionic LLP Hamiltonian which describes a many-body system containing host fermions only. We adapt the self-consistent Hartree-Fock (HF) approach, first proposed by Edwards, to the fermionic LLP Hamiltonian in which a pair of host fermions with momenta  $\mathbf{k}$  and  $\mathbf{k}'$  interact with a potential proportional to  $\mathbf{k} \cdot \mathbf{k}'$ . We apply the HF theory, which has the advantage of not restricting the number of particle-hole pairs, to repulsive Fermi polarons in one dimension. When the impurity and host fermion masses are equal our variational ansatz, where HF orbitals are expanded in terms of free-particle states, produces results in excellent agreement with McGuire's exact analytical results based on the Bethe ansatz. This work raises the prospect of using the HF ansatz and its time-dependent generalization as building blocks for developing all-coupling theories for both equilibrium and nonequilibrium Fermi polarons in higher dimensions.

## I. INTRODUCTION

A polaron is an impurity in a host medium, dressed with excitations of the host medium particles with which it interacts. A polaron may be classified as a Bose polaron or a Fermi polaron depending on whether the host particle excitations obey Bose or Fermi statistics. The idea traces its roots to more than half a century ago when Landau and Pekar [1, 2] likened a conduction electron dressed with phonons (bosons) in an ionic crystal to a polaron. In condensed matter physics, then, polaron studies began with Bose polarons and later spread to impurities submerged in a bath of fermions, e.g. Anderson's orthogonality catastrophe [3, 4], the Kondo effect [5, 6], and the motion of ions in liquid <sup>3</sup>He [7].

The advent of cold atom systems, with their unprecedented flexibility, has greatly heightened the prospect that polaron properties may be explored to great precision across a broad interaction regime and with different dimensionality. The recent renaissance in the study of polarons began with Fermi polarons (see [8, 9] for a review), as cold atom polarons were first realized in experiments with mixtures of highly imbalanced Fermi gases [10, 11]. The results of these experiments were found to be in excellent agreement with earlier theoretical predictions [12–16], which were inspired by experimental realizations of imbalanced mixtures of cold fermionic atoms [17, 18]. This same period also witnessed an increased interest in Bose polarons where the role of the host medium is played by a Bose-Einstein condensate (BEC) [19–25]. In more recent years, there has been a plethora of activity aimed at understanding Fermi polarons both theoretically [26–35] and experimentally [36–40] and Bose polarons both theoretically [41–59] and experimentally [60–62]. As such, polarons continue to be a topic of intense current interest to the cold atom physics community.

Cross-field fertilization has been a hallmark of physics

research. The study of Bose polarons owes its rapid development, in part, to the remarkable progress made in developing and improving our understanding of the Fermi polaron problem in the past decade. For instance, a Chevy-like variational ansatz [12] originally developed for the Fermi polaron problem has been adapted successfully to its bosonic counterpart [46, 52]. In view of recent progress made in the study of Bose polarons, we investigate the opposite scenario where the study of Fermi polarons takes cues from its bosonic cousin.

Specifically we look to the Fröhlich Hamiltonian, popular in the study of Bose polarons, where the impurity is treated, from the outset, as a single-particle quantum system described with canonical position and momentum operators. This may be contrasted with the usual Hamiltonian employed in the study of Fermi polarons, where both impurities and host fermions are described in the language of second quantization for many-body quantum systems. An advantage to using the Fröhlich Hamiltonian is that the Lee-Low-Pine (LLP) transformation [63] can be easily applied, which eliminates the impurity degree of freedom yielding a Hamiltonian describing a single component system with host particles only.

The LLP transformation amounts to changing from the laboratory frame to a moving frame and is therefore a general transformation not limited to Fröhlich Bose polarons. In fact, Edwards [64] recognized years ago for Fermi polarons that moving to a frame attached to the impurity has distinct advantages. Such a change of frame has since found applications in analogous problems across different contexts (see, for example, [65–69]). In both the Bose and the Fermi Fröhlich models, the host particles after the LLP transformation are found to interact with a two-body interaction quite different from the usual two-body interaction. This induced interaction, which is absent in the lab frame, has been the focus of much recent research in Bose polarons [47, 50, 53], which gives

strong support that the LLP transformation in combination with many-body quantum field theory constitutes a powerful tool for developing all-coupling theories for Fröhlich polarons.

In this work, motivated by these latest developments in the study of Bose polarons, we formulate the Fermi polaron problem in a language familiar to the study of Fröhlich polarons involving the use of the LLP transformation with the goal of developing an all coupling theory for Fermi polarons.

In Sec. II, we introduce the fermionic analog of the Fröhlich Hamiltonian, which describes a single spin- $\downarrow$  impurity interacting with *non-interacting* spin- $\uparrow$  fermions, and then apply the LLP transformation to obtain the fermionic LLP model, which describes a spin polarized Fermi system containing *interacting* spin- $\uparrow$  fermions (and free of the impurity degrees of freedom).

In Sec. III, we show that the fermionic LLP model naturally embraces Chevy's ansatz [12], which is a superposition of many-body states with various numbers of particle-hole excitations, as a variational ansatz for weak coupling Fermi polarons.

In Sec. IV, we adapt the Hartree-Fock (HF) variational ansatz, where fermions at equilibrium are assumed to be in a Slater determinant, to the fermionic LLP model of arbitrary dimension. The (HF) ansatz has the advantage that it does not limit the number of particle-hole pairs and is thus expected to be more accurate, particularly in the strong coupling regime, than its perturbative analog presented in Sec. III where the number of particle-hole pairs is fixed a priori.

In Sec. V, we establish the validity of our approach by applying the general theory in Sec. IV to a repulsive Fermi polaron in a quasi-one-dimensional (quasi-1D) setting. For the case where the impurity and host fermion masses are equal, the polaron energy and effective mass are found to be in excellent agreement with McGuire's analytical results [70, 71] based on the Bethe ansatz across a wide range of interaction strengths. We perform an in-depth analysis of the single-particle spectrum in the moving frame, revealing novel features that distinguish weakly-coupled Fermi polarons from strongly-coupled ones. We also discuss and benchmark results where the impurity mass is different from the host fermion mass.

In Sec. VI, we summarize our results and provide further comments about our approach to the Fermi polaron problem.

## II. FERMIONIC POLARON HAMILTONIAN AFTER LEE-LOW-PINE TRANSFORMATION

We start with the Hamiltonian for a two-component Fermi gas mixture in the limit of short-range interactions:

$$\hat{H}' = \sum_{\mathbf{k}} \left( \epsilon_{\mathbf{k}} \hat{a}_{\mathbf{k}}^{\dagger} \hat{a}_{\mathbf{k}} + \epsilon_{\mathbf{k}}^I \hat{c}_{\mathbf{k}}^{\dagger} \hat{c}_{\mathbf{k}} \right) + \frac{g}{\mathcal{V}} \sum_{\mathbf{k}\mathbf{k}'\mathbf{q}} \hat{c}_{\mathbf{k}+\mathbf{q}}^{\dagger} \hat{a}_{\mathbf{k}'-\mathbf{q}}^{\dagger} \hat{a}_{\mathbf{k}'} \hat{c}_{\mathbf{k}}, \quad (1)$$

where  $\mathcal{V}$  is the quantization "volume,"  $g$  is the  $s$ -wave interaction strength between an impurity atom and a host fermion, and  $\hat{a}_{\mathbf{k}}$  and  $\hat{c}_{\mathbf{k}}$  denote, respectively, annihilation operators for a spin- $\uparrow$  majority (host) fermion of mass  $m$  with kinetic energy  $\epsilon_{\mathbf{k}} = k^2/2m$  and a spin- $\downarrow$  minority (impurity) atom of mass  $m_I$  with kinetic energy  $\epsilon_{\mathbf{k}}^I = k^2/2m_I$ , where  $\mathbf{k}$  is the momentum. Taking the so-called single impurity limit, we make the replacements  $\sum_{\mathbf{k}} \hat{c}_{\mathbf{k}+\mathbf{q}}^{\dagger} \hat{c}_{\mathbf{k}} \rightarrow \exp(i\mathbf{q} \cdot \hat{\mathbf{r}})$  and  $\sum_{\mathbf{k}} \epsilon_{\mathbf{k}}^I \hat{c}_{\mathbf{k}}^{\dagger} \hat{c}_{\mathbf{k}} \rightarrow \hat{p}^2/(2m_I)$ , which eliminates the impurity field operators in favor of the impurity position and momentum operators,  $\hat{\mathbf{r}}$  and  $\hat{\mathbf{p}}$ , transforming Eq. (1) into

$$\hat{H}' = \frac{\hat{p}^2}{2m_I} + \sum_{\mathbf{k}} \epsilon_{\mathbf{k}} \hat{a}_{\mathbf{k}}^{\dagger} \hat{a}_{\mathbf{k}} + \frac{g}{\mathcal{V}} \sum_{\mathbf{k},\mathbf{q}} e^{i\mathbf{q} \cdot \hat{\mathbf{r}}} \hat{a}_{\mathbf{k}-\mathbf{q}}^{\dagger} \hat{a}_{\mathbf{k}}, \quad (2)$$

which is the fermionic analog of the well-known Fröhlich Hamiltonian.

The LLP transformation is based upon total momentum conservation. For our Fermi model, a simple evaluation finds  $[\hat{\mathbf{p}}, \hat{H}'] = -[\hat{\mathbf{p}}_f, \hat{H}'] \neq 0$ , indicating that the impurity momentum  $\hat{\mathbf{p}}$  and the total fermion momentum

$$\hat{\mathbf{p}}_f = \sum_{\mathbf{k}} \mathbf{k} \hat{a}_{\mathbf{k}}^{\dagger} \hat{a}_{\mathbf{k}} \quad (3)$$

are not conserved separately but that their sum is conserved,  $[\hat{\mathbf{p}} + \hat{\mathbf{p}}_f, \hat{H}'] = 0$ . This is to be expected since the impurity together with the background fermions forms an isolated system. Just as in the Bose polaron problem, we now introduce the fermionic LLP transformation:

$$\hat{S} = e^{i\hat{\mathbf{r}} \cdot \sum_{\mathbf{k}} \mathbf{k} \hat{a}_{\mathbf{k}}^{\dagger} \hat{a}_{\mathbf{k}}}. \quad (4)$$

A comment regarding the effect of  $\hat{S}$  on vacuum states is in order. For Bose polarons at zero temperature, the vacuum is empty (i.e. free of phonons) and is invariant under the LLP transformation. By contrast, for our Fermi system at zero temperature the "vacuum" is not empty and corresponds to a filled Fermi sea where states below the Fermi energy  $\epsilon_F = k_F^2/2m$  (or Fermi momentum  $k_F$ ) are all occupied. Nevertheless, because the Fermi sea is inert, i.e. the total fermion momentum of the Fermi sea is zero, the Fermi vacuum is also invariant under the LLP transformation. (Unless otherwise stated, by "Fermi sea" we always mean a non-interacting Fermi sea.)

It is easily verified that  $\hat{\mathbf{p}}$  and  $\hat{a}_{\mathbf{k}}$  transform under  $\hat{S}$  analogously to the Bose polaron problem,

$$\hat{S}^{-1} \hat{\mathbf{p}} \hat{S} = \hat{\mathbf{p}} - \sum_{\mathbf{k}} \mathbf{k} \hat{a}_{\mathbf{k}}^{\dagger} \hat{a}_{\mathbf{k}}, \quad (5)$$

$$\hat{S}^{-1} \hat{a}_{\mathbf{k}} \hat{S} = \hat{a}_{\mathbf{k}} e^{-i\mathbf{k} \cdot \hat{\mathbf{r}}}. \quad (6)$$

The Hamiltonian (2) under the LLP transformation,  $\hat{H} = \hat{S}^{-1} \hat{H}' \hat{S}$ , then reads

$$\hat{H} = \frac{\left( \hat{\mathbf{p}} - \sum_{\mathbf{k}} \mathbf{k} \hat{a}_{\mathbf{k}}^{\dagger} \hat{a}_{\mathbf{k}} \right)^2}{2m_I} + \sum_{\mathbf{k}} \epsilon_{\mathbf{k}} \hat{a}_{\mathbf{k}}^{\dagger} \hat{a}_{\mathbf{k}} + \frac{g}{\mathcal{V}} \sum_{\mathbf{k},\mathbf{k}'} \hat{a}_{\mathbf{k}}^{\dagger} \hat{a}_{\mathbf{k}'}, \quad (7)$$

which we refer to as the fermionic LLP Hamiltonian.

The LLP transformation (4) is a Galilean boost operator and can thus be regarded qualitatively as boosting the system into a frame moving at a speed determined by the total fermion momentum. In this frame the impurity momentum  $\hat{\mathbf{p}}$  is a constant of motion allowing it to be replaced with the  $c$ -number  $\mathbf{p}$  in Eq. (7). Comparing the Hamiltonian in Eq. (7) with the Hamiltonian prior to the LLP transformation in Eq. (2), we see that the post-LLP Hamiltonian describes a system containing only fermions, but at the expense of introducing an interaction between them. This is entirely analogous to the LLP transformation in the Bose polaron problem.

### III. PERTURBATIVE VARIATIONAL ANSATZ: CHEVY'S ANSATZ

Polaron problems, be they bosonic or fermionic, are usually studied with variational methods. As a matter of fact, the LLP transformation was originally introduced as a first step towards developing a variational approach to weakly-coupled Fröhlich polarons [63]. To illustrate how the fermionic LLP transformation may inspire variational approaches to weak coupling Fermi polarons, we divide momentum states into particle states  $\mathbf{k}$  with  $|\mathbf{k}| > k_F$  and hole states  $\mathbf{q}$  with  $|\mathbf{q}| < k_F$  and introduce the canonical particle-hole transformation,

$$\hat{b}_{\mathbf{k}} \equiv \hat{a}_{\mathbf{k}}, \quad \hat{b}_{\mathbf{k}}^\dagger \equiv \hat{a}_{\mathbf{k}}^\dagger, \quad \hat{b}_{\mathbf{q}} \equiv \hat{a}_{\mathbf{q}}^\dagger, \quad \hat{b}_{\mathbf{q}}^\dagger \equiv \hat{a}_{\mathbf{q}}, \quad (8)$$

where  $\hat{b}_{\mathbf{k}}$  ( $\hat{b}_{\mathbf{k}}^\dagger$ ) annihilates (creates) a particle with momentum  $\mathbf{k}$  and energy  $\epsilon_{\mathbf{k}}$  and  $\hat{b}_{\mathbf{q}}$  ( $\hat{b}_{\mathbf{q}}^\dagger$ ) annihilates (creates) a hole with momentum  $-\mathbf{q}$  and energy  $-\epsilon_{\mathbf{q}}$ . The application of Eq. (8) changes the LLP Hamiltonian (7) into

$$\hat{H} = \hat{H}_0 + \hat{V}, \quad (9)$$

where

$$\hat{H}_0 = \frac{\left[ \mathbf{p} - \sum_{\mathbf{k}} \mathbf{k} \hat{b}_{\mathbf{k}}^\dagger \hat{b}_{\mathbf{k}} - \sum_{\mathbf{q}} (-\mathbf{q}) \hat{b}_{\mathbf{q}}^\dagger \hat{b}_{\mathbf{q}} \right]^2}{2m_I} + \sum_{\mathbf{q}} \epsilon_{\mathbf{q}} + \sum_{\mathbf{k}} \epsilon_{\mathbf{k}} \hat{b}_{\mathbf{k}}^\dagger \hat{b}_{\mathbf{k}} + \sum_{\mathbf{q}} (-\epsilon_{\mathbf{q}}) \hat{b}_{\mathbf{q}}^\dagger \hat{b}_{\mathbf{q}} \quad (10)$$

follows from the first two terms in Eq. (7) with the final term giving

$$\hat{V} = gn_F \quad (11) + \frac{g}{V} \left( \sum_{\mathbf{k}, \mathbf{k}'} \hat{b}_{\mathbf{k}}^\dagger \hat{b}_{\mathbf{k}'} - \sum_{\mathbf{q}, \mathbf{q}'} \hat{b}_{\mathbf{q}}^\dagger \hat{b}_{\mathbf{q}'} + \sum_{\mathbf{k}, \mathbf{q}} \hat{b}_{\mathbf{k}}^\dagger \hat{b}_{\mathbf{q}}^\dagger - \sum_{\mathbf{k}, \mathbf{q}} \hat{b}_{\mathbf{k}} \hat{b}_{\mathbf{q}} \right),$$

where  $n_F$  is the fermion number density. Here,  $\hat{H}_0$  in Eq. (10) represents the sum of the kinetic energy associated with the impurity recoil (first line) and the free fermion

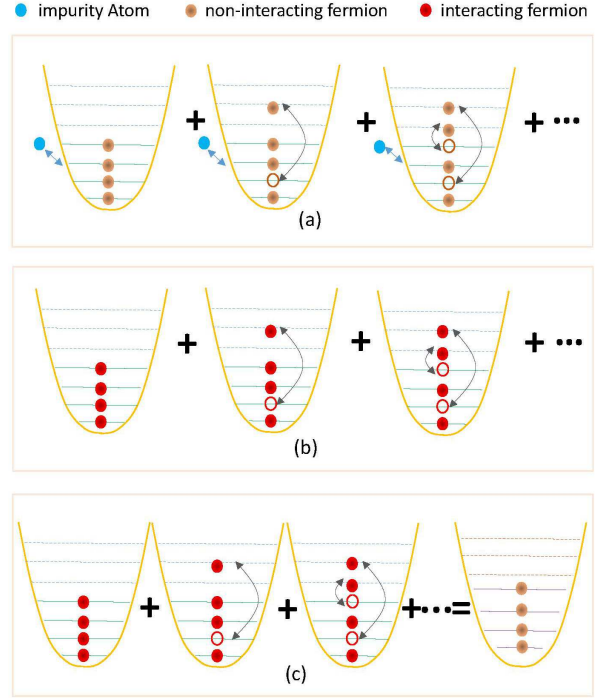


FIG. 1. (a) Chevy's variational ansatz based on the standard second-quantized Hamiltonian (1) in the lab frame. (b) Chevy's variational ansatz based on the LLP Hamiltonian (7) in the moving frame. (c) Self-consistent Hartree-Fock variational ansatz.

energy (second line). A particularly attractive feature of the LLP Hamiltonian (7) is that the  $s$ -wave interaction between an impurity and a host fermion manifests simply as a localized impurity potential,  $g\delta(\mathbf{r})$ , embedded in host fermions.  $\hat{V}$  in Eq. (11) represents this potential scattering.

The eigenstates of  $\hat{H}_0$  are particle-hole excitations. Not only does this fact facilitate the implementation of a perturbation theory in which  $\hat{H}_0$  in Eq. (10) and  $\hat{V}$  in Eq. (11) are treated as the unperturbed Hamiltonian and its perturbation, but it also motivates a variational approach in which a trial wave function is a superposition of families of states grouped according to the number of particle-hole pairs as illustrated in Fig. 1(b). Each term in the  $i$ th family consists of  $i$  particle-hole pairs. For example, the trial wave function up to two particle-hole pairs is

$$|\psi\rangle = \alpha_0 |0\rangle + \sum_{\mathbf{k}\mathbf{q}} \alpha_{\mathbf{k}\mathbf{q}} |1_{\mathbf{k}}1_{\mathbf{q}}\rangle + \frac{1}{(2!)} \sum_{\mathbf{k}\mathbf{k}'\mathbf{q}\mathbf{q}'} \alpha_{\mathbf{k}\mathbf{k}'\mathbf{q}\mathbf{q}'} |1_{\mathbf{k}}1_{\mathbf{k}'}1_{\mathbf{q}}1_{\mathbf{q}'}\rangle, \quad (12)$$

where  $\alpha_0$ ,  $\alpha_{\mathbf{k}\mathbf{q}}$ , and  $\alpha_{\mathbf{k}\mathbf{k}'\mathbf{q}\mathbf{q}'}$  are variational parameters and  $|1_{\mathbf{k}}1_{\mathbf{q}}\rangle \equiv \hat{a}_{\mathbf{k}}^\dagger \hat{a}_{\mathbf{q}} |0\rangle$  and  $|1_{\mathbf{k}}1_{\mathbf{k}'}1_{\mathbf{q}}1_{\mathbf{q}'}\rangle \equiv \hat{a}_{\mathbf{k}}^\dagger \hat{a}_{\mathbf{k}'}^\dagger \hat{a}_{\mathbf{q}} \hat{a}_{\mathbf{q}'} |0\rangle$  are Slater determinants for one and two particle-hole excitations on top of the Fermi sea  $|0\rangle$ .

The same variational expansion for Hamiltonian (1) takes the form

$$|\psi'\rangle = \alpha_0 \hat{c}_{\mathbf{p}}^\dagger |0\rangle + \sum_{\mathbf{k}\mathbf{q}} \alpha_{\mathbf{k}\mathbf{q}} \hat{c}_{\mathbf{p}+\mathbf{q}-\mathbf{k}}^\dagger |1_{\mathbf{k}}1_{\mathbf{q}}\rangle + \frac{1}{(2!)^2} \sum_{\mathbf{k}\mathbf{k}'\mathbf{q}\mathbf{q}'} \alpha_{\mathbf{k}\mathbf{k}'\mathbf{q}\mathbf{q}'} \hat{c}_{\mathbf{p}+\mathbf{q}+\mathbf{q}'-\mathbf{k}-\mathbf{k}'}^\dagger |1_{\mathbf{k}}1_{\mathbf{k}'}1_{\mathbf{q}}1_{\mathbf{q}'}\rangle, \quad (13)$$

which is Chevy's celebrated ansatz first introduced by Chevy for one particle-hole pair [12] and subsequently generalized to higher particle-hole pairs [15]. Figure 1(a) illustrates the expansion used to construct the trial wave function (13).

Because particle-hole excitations, such as  $|1_{\mathbf{k}}1_{\mathbf{q}}\rangle$ , are eigenstates of the total fermion momentum, one can show that Chevy's ansatz (13) transforms under the LLP transformation as

$$\hat{S}|\psi'\rangle = |\mathbf{p}\rangle \otimes |\psi\rangle, \quad (14)$$

which is the direct product of  $|\mathbf{p}\rangle$ , an impurity state with total momentum  $\mathbf{p}$ , and  $|\psi\rangle$  in Eq. (12), our trial wave function for host fermions only, demonstrating again that the LLP transformation decouples the impurity from the host fermions.

The necessity to terminate the expansion as in our example in Eq. (12) can be traced to  $\hat{V}$  in Eq. (11). The term in the top line shifts the mean-field energy. In the second line the first term couples particle states and the second term couples hole states, both of which couple within the *same* particle-hole family. The final two terms on the last line couple *different* families through particle-hole creation (third term) and particle-hole annihilation (fourth term) and it is these couplings (across different families) that make it necessary to restrict the number of particle-hole pairs in the trial wave function so that the problem can be described by a closed set of equations.

#### IV. NON-PERTURBATIVE ALL-COUPLED VARIATIONAL ANSATZ: SELF-CONSISTENT HARTREE-FOCK ANSATZ

A Fermi polaron is simply an impurity clothed with particle-hole excitations. In order to yield a more accurate polaron description, efforts were made early on to construct nonperturbative variational ansatzes which do not restrict the number of particle-hole excitations [14, 15]. Here, we aim to achieve this goal by using an approach inspired in large part by recent advancements in the study of Bose polarons [47, 50, 53]. We begin by casting Eq. (7) into the normally-ordered form

$$\hat{H} = \frac{p^2}{2m_I} + \frac{g}{V} \sum_{\mathbf{k},\mathbf{k}'} \hat{a}_{\mathbf{k}}^\dagger \hat{a}_{\mathbf{k}'} + \sum_{\mathbf{k}} \left( \epsilon_{\mathbf{k}} + \epsilon_{\mathbf{k}}^I - \frac{\mathbf{k} \cdot \mathbf{p}}{m_I} \right) \hat{a}_{\mathbf{k}}^\dagger \hat{a}_{\mathbf{k}} + \hat{H}_{\text{int}}. \quad (15)$$

As in the Bose case, the LLP Hamiltonian (15) distinguishes itself with a quartic interaction term,

$$\hat{H}_{\text{int}} = \frac{1}{2m_I} \sum_{\mathbf{k},\mathbf{k}'} (\mathbf{k} \cdot \mathbf{k}') \hat{a}_{\mathbf{k}}^\dagger \hat{a}_{\mathbf{k}'}^\dagger \hat{a}_{\mathbf{k}'} \hat{a}_{\mathbf{k}}, \quad (16)$$

which indicates that a pair of host particles with momenta  $\mathbf{k}$  and  $\mathbf{k}'$ , which are non-interacting in the lab frame, interact in the moving frame with an interaction potential linearly proportional to  $\mathbf{k} \cdot \mathbf{k}'$  but inversely proportional to the impurity mass  $m_I$ .

Usually systems described by the LLP Hamiltonian, owing to  $\hat{H}_{\text{int}}$  being quartic, cannot be solved exactly. Thankfully there exist a rich set of field theoretic techniques for solving (approximately) many-body quantum systems containing four-fermion interactions [6]. In this paper, we circumvent complications arising from the LLP induced Fermi-Fermi interaction (16) by adapting the Hartree-Fock (HF) treatment to the LLP Hamiltonian in Eq. (15) at zero temperature. Note that the  $T$ -matrix approximation involving the use of ladder diagrams, a field theoretical technique, was used in the study of polarons described by the original Hamiltonian (1) [14], but there the use of the technique was made for a very different reason—to combat difficulties arising from the impurity-fermion interaction which is quartic in the original Hamiltonian (1).

The essence of the HF approach is summarized as follows. For a free Fermi gas, the many-body ground state (Fermi sea) is a Slater determinant of the lowest single-particle momentum states  $|\mathbf{k}\rangle$  up to the Fermi energy  $\epsilon_F = k_F^2/2m$  with  $k_F$  the Fermi momentum. The HF approximation amounts to assuming that for an interacting Fermi gas, the many-body ground state  $|\phi\rangle$  continues to be in a Slater determinant but composed of a set of orthonormal single-particle orbitals  $|n\rangle$ , known as Hartree-Fock orbitals, up to the chemical potential  $\mu$ .

Edwards proposed this ansatz in the position representation [64], inspired by the wave function introduced by Wigner and Seitz in their discussion of electron correlations in sodium [72]. Instead, we formulate the theory in a manner parallel to our recent work for Fröhlich polarons [53] except that pair correlations, which are important in Bose polaron systems [47, 50, 53], are excluded because of the lack of superfluidity in our Fermi model. Note that our Hamiltonian in Eq. (1) is for a wide Feshbach resonance characterized by a single parameter—the  $s$ -wave scattering length. As such our HF ansatz can describe the polaron-molecule crossover; it cannot capture three-body physics where parameters besides the  $s$ -wave scattering length are required to describe the impurity-host fermion interaction.

As with our earlier study [53], instead of single-particle orbitals, we find it more convenient to work with the (Hermitian) single-particle density matrix  $\rho$  associated with  $|\phi\rangle$ , defined as

$$\rho_{\mathbf{k}\mathbf{k}'} = \langle \phi | \hat{a}_{\mathbf{k}}^\dagger \hat{a}_{\mathbf{k}} | \phi \rangle. \quad (17)$$

The average energy,  $E \equiv \langle \phi | \hat{H} | \phi \rangle$ , for a system prepared in state  $|\phi\rangle$  is then a functional of  $\rho$  given by

$$E = \frac{p^2}{2m_I} + \sum_{\mathbf{k}} \left( \epsilon_{\mathbf{k}} + \epsilon_{\mathbf{k}}^I - \frac{\mathbf{k} \cdot \mathbf{p}}{m_I} \right) \rho_{\mathbf{k}\mathbf{k}} + \frac{g}{\mathcal{V}} \sum_{\mathbf{k}, \mathbf{k}'} \rho_{\mathbf{k}\mathbf{k}'} + \sum_{\mathbf{k}, \mathbf{k}'} \frac{\mathbf{k} \cdot \mathbf{k}'}{2m_I} \left( \rho_{\mathbf{k}\mathbf{k}} \rho_{\mathbf{k}'\mathbf{k}'} - |\rho_{\mathbf{k}\mathbf{k}'}|^2 \right), \quad (18)$$

where the term proportional to  $\rho_{\mathbf{k}\mathbf{k}} \rho_{\mathbf{k}'\mathbf{k}'}$  is due to the Hartree contribution and the  $-|\rho_{\mathbf{k}\mathbf{k}'}|^2$  term follows from the Fock exchange contribution. Note that for  $\rho$  to represent a Slater determinant it must satisfy

$$\rho^2 = \rho. \quad (19)$$

Minimizing  $E$  in Eq. (18) with respect to  $\rho$  subject to condition (19), i.e.

$$\delta (E - Tr [\Lambda (\rho^2 - \rho)]) = 0, \quad (20)$$

we arrive at the HF equation,

$$[A, \rho] = 0, \quad (21)$$

where  $\Lambda$  is a matrix of Lagrange multipliers associated with constraint (19) and  $A$  is a matrix defined as  $A_{\mathbf{k}\mathbf{k}'} = \partial E / \partial \rho_{\mathbf{k}'\mathbf{k}}$  or explicitly

$$A_{\mathbf{k}\mathbf{k}'} = \left[ \epsilon_{\mathbf{k}} + \epsilon_{\mathbf{k}}^I - \frac{\mathbf{k} \cdot (\mathbf{p} - \mathbf{p}_f)}{m_I} \right] \delta_{\mathbf{k}, \mathbf{k}'} + \frac{g}{\mathcal{V}} - \frac{\mathbf{k} \cdot \mathbf{k}'}{m_I} \rho_{\mathbf{k}\mathbf{k}'}, \quad (22)$$

with

$$\mathbf{p}_f = \sum_{\mathbf{k}} \mathbf{k} \langle \phi | \hat{a}_{\mathbf{k}}^\dagger \hat{a}_{\mathbf{k}} | \phi \rangle = \sum_{\mathbf{k}} \mathbf{k} \rho_{\mathbf{k}\mathbf{k}} \quad (23)$$

being the total fermion momentum.

The HF equation (21) is automatically satisfied when one chooses the HF orbital  $|n\rangle$  as the eigenstate of  $A$ :

$$A |n\rangle = \omega_n |n\rangle, \quad (24)$$

where  $\omega_n$  is the eigenvalue and

$$|n\rangle = \sum_{\mathbf{k}} U_{\mathbf{k}n} |\mathbf{k}\rangle, \quad (25)$$

is the corresponding eigenstate normalized according to

$$\sum_{\mathbf{k}} |U_{\mathbf{k}n}|^2 = 1. \quad (26)$$

The density matrix  $\rho$  is then constructed as the projector onto the space spanned by occupied orbitals  $\{|n\rangle\}$ :

$$\rho = \sum_n |n\rangle \langle n| \theta(\mu - \omega_n), \quad (27)$$

where the step function  $\theta(\mu - \omega_n)$  is introduced to impose the Pauli exclusion principle at zero temperature.

Equation (24) is the momentum space representation of Edward's position space HF equations [64].

In the actual numerical implementation, the single-particle HF orbital  $|n\rangle$  has to be determined iteratively (starting, in our implementation, by assuming fermions in a Fermi sea). This is because Eq. (24) is a nonlinear equation; matrix  $A$  is itself a function of  $|n\rangle$  via the density matrix element in Eq. (22),

$$\rho_{\mathbf{k}\mathbf{k}'} = \sum_n U_{\mathbf{k}n}^* U_{\mathbf{k}'n} \theta(\mu - \omega_n), \quad (28)$$

where the chemical potential  $\mu$  is fixed by the fermion number conservation law,

$$n_F = \frac{1}{\mathcal{V}} \sum_{\mathbf{k}} \rho_{\mathbf{k}\mathbf{k}}, \quad (29)$$

with  $n_F$  the background fermion number density. This simple iterative procedure can only lead to the ground state and therefore cannot capture phenomena associated with excited states such as the Fermi super-Tonks state [73].

The HF method amounts to moving from  $\{|\mathbf{k}\rangle\}$  space where  $A$  has the matrix representation (22) to  $\{|n\rangle\}$  space where  $A$  is diagonalized through a unitary transformation  $U$ , with  $U_{\mathbf{k}n} = \langle \mathbf{k} | n \rangle$  defined in Eq. (25). This unitary transformation induces a linear mapping between field operators in the two spaces,

$$\hat{d}_n = \sum_{\mathbf{k}} \hat{a}_{\mathbf{k}} U_{\mathbf{k}n}, \quad (30)$$

which defines the quasiparticle field operator  $\hat{d}_n$  in  $\{|n\rangle\}$  space. The many-body HF state  $|\phi\rangle$ , when viewed in  $\{|n\rangle\}$  space, contains neither quasiparticles nor quasiholes, i.e. it is a vacuum with respect to both  $\hat{d}_n$  with  $\omega_n > \mu$  and  $\hat{d}_n^\dagger$  with  $\omega_n < \mu$ . But, when viewed in  $\{|\mathbf{k}\rangle\}$  space  $|\phi\rangle$  is a superposition of terms with different numbers of particle-hole pair excitations (relative to the Fermi sea in  $\{|\mathbf{k}\rangle\}$  space). In contrast to the trial state expansion in the weak coupling theory which includes terms only up to a limited number of particle-hole pairs, the trial state  $|\phi\rangle$  in the HF theory, when expanded, consists of an unrestricted number of particle-hole pairs as illustrated in Fig. 1(c). In fact, the HF equation adjusts particle-hole pairs by itself according to the impurity-fermion interaction strength and the impurity-fermion mass ratio. Thus, the self-consistent HF theory is a nonperturbative variational approach that is expected to perform well even in the limit of strong impurity-fermion coupling.

The polaron energy (at momentum  $\mathbf{p}$ ) is the total energy  $E$  in Eq. (18) relative to the energy of the Fermi sea,  $\sum_{\mathbf{k}} \epsilon_{\mathbf{k}} \theta(\epsilon_F - \epsilon_{\mathbf{k}})$ , which simplifies when Eqs. (24) and (27) are taken into consideration to

$$E_p = \mathcal{E}_0 + \sum_n \omega_n \theta(\mu - \omega_n) - \sum_{\mathbf{k}} \epsilon_{\mathbf{k}} \theta(\epsilon_F - \epsilon_{\mathbf{k}}), \quad (31)$$

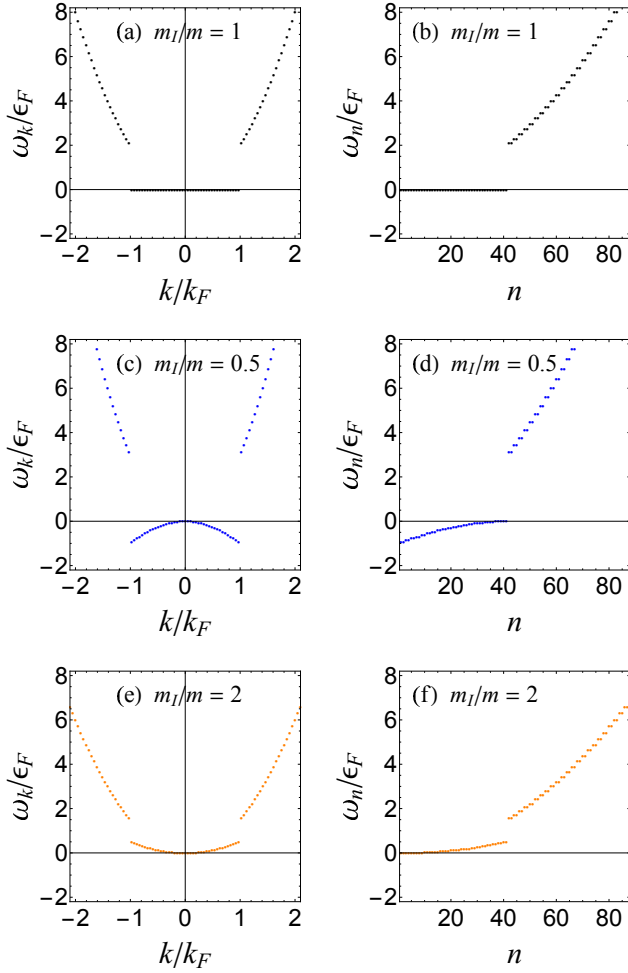


FIG. 2. (Color online.) The HF single-particle energy spectrum for free fermions in a one-dimensional Fermi sea ( $g = p = 0$ ) as seen in the moving (LLP) frame as a function of  $k$  (left column) and as a function of energy quantum number  $n$  (right column) when  $m_I/m = 1$  (top row, black), 0.5 (middle row, blue), and 2 (bottom row, orange). These and all subsequent figures were made with a momentum cutoff of  $25k_F$ .

where

$$\mathcal{E}_0 = \frac{p^2}{2m_I} - \frac{p_f^2}{2m_I} + \frac{1}{2} \sum_{\mathbf{k}, \mathbf{k}'} \frac{\mathbf{k} \cdot \mathbf{k}'}{m_I} |\rho_{\mathbf{k}\mathbf{k}'}|^2. \quad (32)$$

For  $\mathbf{p}$  near zero, Eq. (31) takes the approximate form  $E_p \approx E_0 + p^2/2m_I^*$ , where  $E_0$  is the ground state polaron energy ( $p = 0$ ) and

$$m_I^* = \left. \frac{\partial^2 E_p}{\partial p^2} \right|_{p=0} \quad (33)$$

is defined as the effective impurity mass, which, because of momentum conservation, is equivalent to

$$m_I^* = \left( \frac{1}{m_I} - \frac{1}{m_I} \lim_{p \rightarrow 0} \frac{\mathbf{p}_f \cdot \mathbf{p}}{p^2} \right)^{-1}. \quad (34)$$

The central task of the HF approach is to solve Eq. (24) self consistently for single-particle eigenenergies and corresponding eigenvectors. The single-particle energy spectrum in the moving (LLP) frame of reference (and within the HF approximation), as determined from Eq. (24), is expected to look drastically different from that in the lab frame. As preparation for a detailed study in the next section, we conclude this section using the Fermi sea as an example to clarify this point. The Fermi sea in the lab frame is filled with fermions with free particle dispersion  $\epsilon_{\mathbf{k}}$ . In contrast, the same Fermi sea in the moving frame is occupied by fermions with a quite different energy dispersion:

$$\omega_{\mathbf{k}} = \begin{cases} \epsilon_{\mathbf{k}} - \epsilon_{\mathbf{k}}^I & \text{if } |\mathbf{k}| < k_F \\ \epsilon_{\mathbf{k}} + \epsilon_{\mathbf{k}}^I & \text{if } |\mathbf{k}| > k_F, \end{cases} \quad (35)$$

which we obtained by describing the Fermi sea using density matrix  $\rho_{\mathbf{k}\mathbf{k}'} = \delta_{\mathbf{k},\mathbf{k}'} \theta(\epsilon_F - \epsilon_{\mathbf{k}})$ . This is shown in the left column of Fig. 2, where an energy jump of width  $2\epsilon_{k_F}^I = k_F^2/m_I$  at  $k = \pm k_F$  can be seen. Only in the heavy impurity limit,  $m_I = \infty$ , does this discontinuity vanish and do the single-particle dispersions in the lab and moving frames agree. The energy spectrum in  $\{|n\rangle\}$  space is shown in the right column in Fig. 2 where the energy jump at the Fermi surface has a width  $2\epsilon_{k_F}^I$  for  $m_I > m$  and  $\epsilon_{k_F} + \epsilon_{k_F}^I$  for  $m_I < m$ .

## V. DISCUSSION: 1D SYSTEM

In this section we specialize the HF polaron theory to a quasi-1D (1D) system where sufficiently high harmonic trap potentials along the transverse dimension are employed to confine the motion of atoms to zero-point oscillations. The effective 1D coupling constant  $g$  can be tuned from negative to positive via confinement-induced resonance [74, 75]. The precise value of  $g$  in 1D can be obtained from the corresponding 3D scattering length following well-established recipes, regardless of whether the impurity and host fermions experience the same [74] or different [76] trap frequencies. Not only is this 1D model of fundamental importance in its own right (see, for example, [77] for a review), but it also affords us a proof-of-principle opportunity to test our HF theory. First, the 1D model, unlike its 2D and 3D counterparts, does not suffer from ultraviolet divergences and therefore is not in need of being renormalized before application of our theory. Second, there exists an exact analytical solution due to McGuire [70, 71] for the case of equal masses  $m_I = m$ . Third, a detailed study based on Chevy's ansatz is available in the literature [78], which serves as another important benchmark against which our approach can be compared.

The Hartree-Fock ansatz can accommodate both positive and negative  $g$ . In order to focus on the role of particle-hole excitations in polaron physics, in what follows we limit our study to models with a (strong) positive  $g$ . Models with a (strong) negative  $g$  are known to

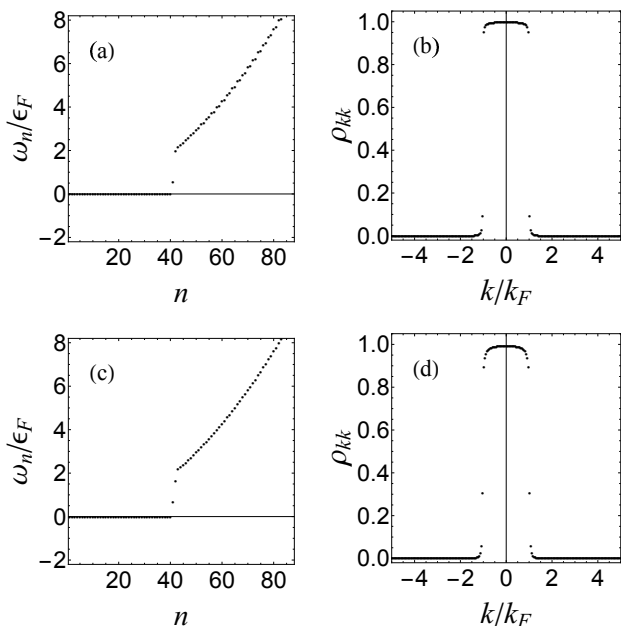


FIG. 3. The single-particle energy spectrum  $\omega_n$  (left column) and momentum distribution  $\rho_{\mathbf{k}\mathbf{k}}$  (right column) for equal masses  $m_I/m = 1$  when  $gm/2k_F = 1$  (top row) and 5 (bottom row).

be dominated by a bound state [78] whose study we leave for future work.

#### A. Equal Masses: $m_I = m$

Consider first the case where the impurity and host fermion masses are equal,  $m_I = m$ , which, according to Eq. (35), features a Fermi sea where all occupied states are degenerate with zero energy and the discontinuity at the Fermi surface has a width twice as large as the Fermi energy  $\epsilon_F$ , as illustrated in the  $m_I/m = 1$  curve in Fig. 2(a). Figure 2(b) shows the single-particle spectrum in  $\{|n\rangle\}$  space where it has a two-fold degeneracy due to inversion symmetry. Note that no states exist inside the discontinuity.

If we increase  $g$  we see in Fig. 3(a) that the state directly below the discontinuity (i.e. directly below the Fermi surface) breaks away from the Fermi sea and enters the gap. The chemical potential is determined by this break-away state, which changes from 0 (when  $g = 0$ ) to a finite value proportional to  $g$ . In addition, the two-fold degeneracy for  $g = 0$  is lifted by the anisotropy of the effective two-body interaction (16). If we increase  $g$  further we see in Fig. 3(c) that the state directly above the discontinuity now breaks away and joins the state that broke away from below, forming an energy spectrum characterized by two “in-gap” states.

Important to Fermi polaron physics is the level of particle-hole activity. Focus now on the momentum distribution in Figs. 3(b) and (d). We see that increasing

the impurity-fermion interaction  $g$  tends to reduce the sharpness of  $\rho_{\mathbf{k}\mathbf{k}}$  and hence, as expected, increase the particle-hole excitations near the Fermi surface.

These features of the energy spectrum  $\omega_n$  (i.e. two “in-gap” states) and the momentum distribution  $\rho_{\mathbf{k}\mathbf{k}}$  are found to remain essentially the same as  $g$  is further increased, implying that the system saturates, which is known to occur in 1D models in the strong repulsive limit  $g \rightarrow +\infty$  [78].

McGuire, using the Bethe ansatz (BA) [79], showed that the Fermi polaron model with equal masses is integrable [70, 71]. McGuire’s work was the catalyst that led Yang [80] and Gaudin [81] to the exact solution for 1D Fermi gases and Lieb and Wu [82] to the exact solution of the 1D Hubbard model with arbitrary spin population imbalance. McGuire’s treatment also motivated Edwards [64] to expand the HF orbital  $|n\rangle$  for a system of  $N$  fermions in terms of  $N + 1$  plane-wave states  $|k_t\rangle$ :

$$|n\rangle = \sum_{t=0}^N a_{nt} |k_t\rangle, \quad n = 1, 2, \dots, N, \quad (36)$$

where the momenta  $k_t$  are given by the BA-like equations

$$\mathcal{V}k_t = 2\pi n_t - 2\delta_t \quad (37)$$

and

$$\delta_t = -\pi s \operatorname{sgn}(k_t) / 2 + \tan^{-1} [(2k_t - \Lambda) / mg], \quad (38)$$

with  $n_t$  an integer and  $\Lambda$  the spectral parameter fixed by the total momentum  $p = \sum_{t=0}^N k_t$ . Expanding the polaron energy

$$E_p = \sum_{t=0}^N \frac{k_t^2}{2m} - \sum_{\mathbf{k}} \epsilon_{\mathbf{k}} \theta(\epsilon_F - \epsilon_{\mathbf{k}}) \quad (39)$$

up to second order in  $p$  leads to McGuire’s analytical results for the polaron energy

$$E_0 = \frac{2\epsilon_F}{\pi} \left[ \bar{g} - \frac{\pi}{2} \bar{g}^2 + (1 + \bar{g}^2) \tan^{-1} \bar{g} \right] \quad (40)$$

and the effective mass

$$m_I^* = m \frac{(1 - \frac{2}{\pi} \tan^{-1} \bar{g})^2}{1 - \frac{2}{\pi} \left( \tan^{-1} \bar{g} + \frac{\bar{g}}{1 + \bar{g}^2} \right)}, \quad (41)$$

where  $\bar{g} = gm/2k_F$  is a unitless quantity measuring the interaction strength.

McGuire’s exact analytical results for  $m_I = m$ , then, afford an excellent opportunity for to test our model. Figures 4(a) and 4(b) display, respectively, the polaron energy and effective polaron mass as functions of the impurity-fermion interaction strength  $g$ . The results computed using our HF theory (solid lines) are seen to be in remarkable agreement with McGuire’s exact analytical solutions (dashed lines). That our polaron energy is slightly higher than McGuire’s is not unexpected since

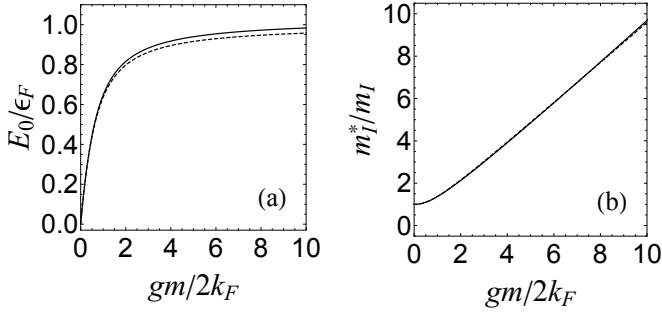


FIG. 4. (a) Polaron energy  $E_0$  and (b) effective polaron mass  $m_I^*$ , both as functions of  $g$  and for equal masses  $m_I = m$  (and for  $p = 0$ ). Solid curves are from our HF theory and dotted curves are McGuire's exact results.

our ansatz is a variational one—so that we may apply our theory to situations with  $m_I \neq m$ , where states similar to  $|k_t\rangle$  do not exist, we expanded the HF orbital in Eq. (25) in terms of the usual free-particle states whose wave vector  $k$  is different from  $k_t$  used in the BA equations which is modified by the impurity-fermion scattering.

### B. Arbitrary Mass Impurity

Having conducted a detailed comparison for the equal mass case, we now turn our attention to the cases where the impurity mass is not equal to the host particle mass,  $m_I \neq m$ .

Figure 5 displays typical single-particle spectra (left column) and momentum distributions (right column) for a lighter impurity  $m_I < m$  (top two rows) and for a heavier impurity  $m_I > m$  (bottom two rows).

Below the Fermi surface, the light impurity spectrum is negative and concave while the heavy impurity spectrum is positive and convex. At the Fermi surface, the former exhibits a larger jump while the latter exhibits a smaller jump compared to the equal mass case in Fig. 3. The features inside the discontinuity remains qualitatively the same as those for equal masses, i.e. as  $g$  increases there emerges first one and then two isolated states.

The momentum distributions in the right column in Fig. 5 agree with our physical intuition based on the LLP induced Fermi-Fermi interaction (16), namely, for a given  $g$  a heavier impurity suppresses while a lighter impurity enhances particle-hole activities compared to the equal mass case in Fig. 3.

Figure 6 shows the polaron energies and effective masses as functions of  $g$  for lighter impurities (top row) and heavier impurities (bottom row). For large  $g$  the polaron energy plateaus while the effective mass continues to increase, just as in the equal mass case.

For small  $g$ ,  $E_0$  and  $m_I^*$  are found to increase according to perturbation theory in which  $\hat{V}$  in Eq. (11) is treated as a perturbation to  $\hat{H}_0$  in Eq. (10). Let  $E_0^{(0)}$  and  $E_{\mathbf{k}\mathbf{q}}^{(1)}$  be, respectively, the eigenenergies of the eigenstates  $|0\rangle$

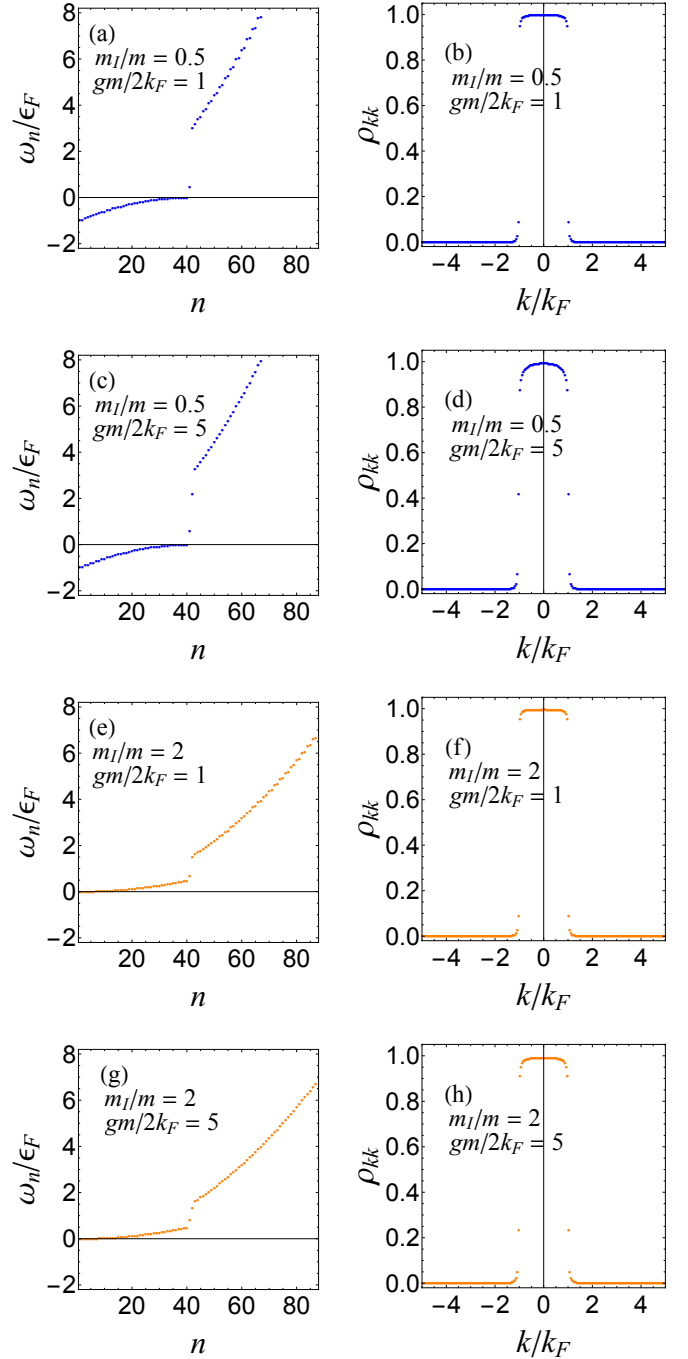


FIG. 5. HF single-particle energy spectrum  $\omega_n$  (left column) and momentum distribution  $\rho_{\mathbf{k}\mathbf{k}}$  (right column) for  $m_I/m = 0.5$  (top two rows) and 2 (bottom two rows) and  $gm/2k_F = 1$  (first and third rows) and 5 (second and fourth rows).

and  $|1_{\mathbf{k}}1_{\mathbf{q}}\rangle$  of  $\hat{H}_0$ . The polaron energy  $E_p$  up to second order in  $g$  is given by

$$E_p = \frac{p^2}{2m_I} + \langle 0 | \hat{V} | 0 \rangle + \sum_{\substack{\mathbf{q} < k_F \\ \mathbf{k} > k_F}} \frac{|\langle 0 | \hat{V} | 1_{\mathbf{k}}1_{\mathbf{q}} \rangle|^2}{E_0^{(0)} - E_{\mathbf{k}\mathbf{q}}^{(1)}} \quad (42)$$



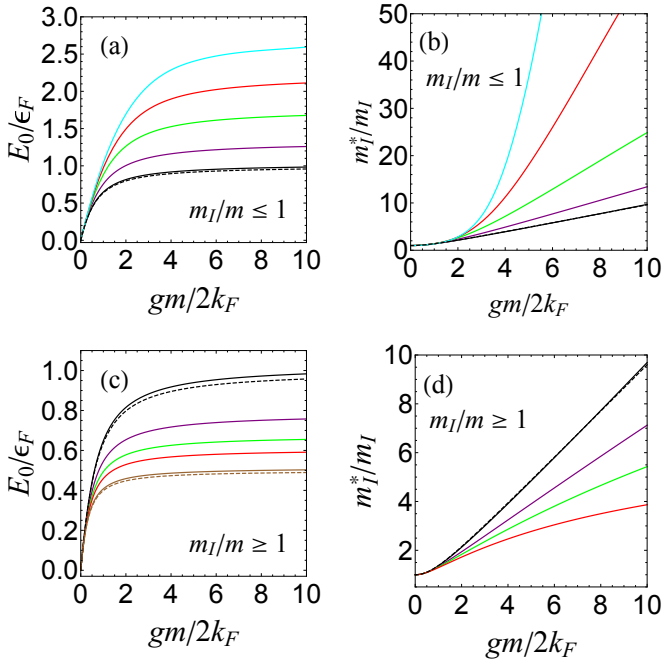


FIG. 6. (Color online.) Polaron energy  $E_0$  (first column) and effective mass  $m_I^*$  (second column). The top row is for an impurity mass lighter than or equal to the host fermion mass. From bottom to top  $m_I/m = 1$  (black), 0.5 (purple), 0.25 (green), 0.15 (red), and 0.1 (cyan). The dashed lines are McGuire's exact results in Eqs. (40) and (41). The bottom row is for an impurity mass heavier or equal to the host fermion mass. From top to bottom  $m_I/m = 1$  (black), 2.5 (purple), 5 (green), and 10 (red). The bottom (brown) curve in (a) is the polaron energy for  $m_I/m = \infty$ . Dashed lines are again exact results, Eqs. (40) and (41) for  $m_I/m = 1$  and Eq. (48) for  $m_I/m = \infty$ .

or explicitly

$$E_p = \frac{p^2}{2m_I} + gn_F - 2\frac{g^2 m_I}{(2\pi)^2} \times \int \int \frac{dqdk}{q-k} \frac{1}{2p+q-k - \frac{m_I}{m}(q+k)}, \quad (43)$$

which yields the polaron energy

$$E_0 = \frac{4}{\pi} \epsilon_F \bar{g} \left[ 1 - \frac{\bar{g}}{\pi} \left( \frac{\pi^2}{4} + \text{Li}_2(\alpha) - \text{Li}_2(-\alpha) \right) \right] \quad (44)$$

[78] and the effective mass

$$\frac{m_I^*}{m_I} = 1 + \frac{4}{\pi^2} (1 + \alpha)^2 \bar{g}^2 \quad (45)$$

up to second order in  $g$ , where  $\text{Li}_2(\alpha)$  is the dilogarithm function and  $\alpha = (m_I - m)/(m_I + m)$ .

The polaron energies for lighter impurities in Fig. 6(a) lie above the bottom curve for equal masses. The lighter the impurity, the stronger the LLP induced interaction (16) and hence the higher the polaron energy. In addition, the kinetic energy from impurity recoil, and hence

$\hat{H}_0$  in Eq. (10), increases with  $\hat{V}$  in Eq. (11) when the impurity mass decreases. Thus the lighter the impurity, the larger the domain  $g$  upon which the perturbative expansions in Eqs. (44) and (45) become valid; these perturbative expansions become exact in the zero impurity mass limit.

The polaron energies for heavier impurities in Fig. 6(c) lie between the top curve for equal masses and the bottom one for a localized impurity (i.e.  $m_I = \infty$ ). The polaron energy for a localized impurity arises solely from the scattering of host fermions by a Dirac delta potential  $g\delta(\mathbf{r})$ . It can be found analytically in 1D analogously to how it is done in 3D by enclosing the impurity (at the origin) between  $-R$  and  $+R$  and analyzing the phase shift in the thermodynamic limit  $R \rightarrow \infty$  [78]. This is identical to the set-up in which one derives Fumi's theorem [4],

$$E_0 = - \int_0^{\epsilon_F} \frac{\eta(\epsilon)}{\pi} d\epsilon. \quad (46)$$

When applied to a 1D system where the phase depends on the energy  $\epsilon$  according to

$$\eta(\epsilon) = - \tan^{-1} \left( g \sqrt{\frac{m}{2\epsilon}} \right), \quad (47)$$

Fumi's theorem yields the polaron energy

$$E_0 = \frac{\epsilon_F}{\pi} \left[ 2\bar{g} - \frac{\pi}{2} (2\bar{g})^2 + \left( 1 + (2\bar{g})^2 \right) \tan^{-1} (2\bar{g}) \right]. \quad (48)$$

The bottom most dashed curve in Fig. 6(c) displays Eq. (48). Note that our ansatz (25) for expanding the HF orbital  $|n\rangle$  in terms of the usual free-particle states becomes exact (without having to resort to the HF approximation) for an infinitely heavy impurity. The slight difference between our result and Eq. (48) is due solely to finite size effects.

We end this section with Table I which displays polaron energies for various impurity masses and interaction strengths computed using our self-consistent HF method.

## VI. CONCLUSION

The Fröhlich Hamiltonian and the LLP transformation have played important roles in advancing our understanding of Bose polarons. We applied the same techniques to transform the Fermi polaron problem to the fermionic LLP model which contains only host fermions, but that interact with each other. We adapted the variational principle based on the HF approximation to the fermionic LLP Hamiltonian. We applied this HF theory, which has the advantage of not imposing restrictions on the number of particle-hole pairs, to repulsive Fermi polarons in one dimension. The polaron properties depend crucially on the single-particle energy spectrum

$gm/2k_F$ \ $m_I/m$	0.1	1	10	50	100
0.1	0.125	1.04	2.56	2.68	2.70
0.5	0.121	0.756	1.26	1.31	1.32
1	0.118 (0.118)	0.648 (0.637)	0.983 (0.958)	1.02 (0.992)	1.02 (0.996)
2	0.116	0.566	0.801	0.826	0.829
10	0.112	0.459	0.591	0.604	0.605
$\infty$	0.110 (0.109)	0.408 (0.399)	0.503 (0.489)	0.512 (0.498)	0.513 (0.499)

TABLE I. Various polaron energies,  $E_0/\epsilon_F$ , for impurities with mass  $m_I$  and strength of interaction with host fermions  $g$ . Numbers in parentheses are exact analytical results from Eqs. (40) and (48).

which features a jump at the Fermi surface in the moving frame. We discovered that as the impurity-fermion interaction increases, the spectrum changes from having one isolated state to having two isolated states inside the discontinuity. We found that, for the case where impurity and host fermion masses are equal, our results calculated from the HF variational ansatz are in excellent agreement with McGuire’s exact solution from the Bethe ansatz. Finally, we used the HF theory to compute the polaron energy for impurities with different masses and interaction strengths. For the remainder of this conclusion we highlight additional merits of our approach to the Fermi polaron problem.

In addition to the polaron energy and effective mass, polaron systems can be characterized by various correlation functions, which can be probed in cold atom experiments using, for example, time-of-flight [83–85] and radio-frequency spectrum techniques [86, 87]. Describing a Fermi polaron system using a Slater determinant involving HF orbitals can significantly simplify the task of calculating these correlation functions, something known

to be difficult to do using the Bethe ansatz.

A great impetus for the recent flood of activity in nonequilibrium polaron dynamics (see, for example, [35] and references therein) is that coherent dynamics, which often changes too rapidly to be directly observed in solid state systems, can be studied in real time using techniques such as Ramsey interferometry in cold atom systems [39]. The HF polaron theory we developed in this work has its nonequilibrium analog—the time-dependent HF variational principle. Thus, we consider it a strength of our approach that it can be adapted straightforwardly to nonequilibrium polaron problems.

Finally, casting the Fermi polaron problem in a moving frame has the advantage that many-body field theoretic tools other than HF methods may also be applied to solve the problem [6]. In particular, it remains an interesting question whether renormalization group techniques, similar to those recently developed by Fabian et al. [47, 56, 88], can be developed to improve our understanding of strongly-coupled Fermi polarons in higher dimensions.

- 
- [1] S. I. Pekar, Zh. Eksp. Teor. Fiz. **16** 341 (1946).  
[2] L. D. Landau and S. I. Pekar, Zh. Eksp. Teor. Fiz **18**, 419 (1948).  
[3] P. W. Anderson, Phys. Rev. Lett. **18**, 1049 (1967),  
[4] G. D. Mahan, Kluwer Academic/Plenum Publishers, New York (2000).  
[5] J. Kondo, Progress of Theoretical Physics **32**, 37 (1964),  
[6] A. C. Hewson, Cambridge University Press, Cambridge, UK (1997).  
[7] J. Kondo and T. Soda, Journal of Low Temperature Physics **50**, 21 (1983),  
[8] F. Chevy and C. Mora, Rep. Prog. Phys. **73**, 112401 (2010).  
[9] P. Massignan, M. Zaccanti, and G. M. Bruun, Reports on Progress in Physics **77**, 034401 (2014),  
[10] A. Schirotzek, C.-H. Wu, A. Sommer, and M. W. Zwierlein, Phys. Rev. Lett. **102**, 230402 (2009).  
[11] S. Nascimbène, N. Navon, K. J. Jiang, L. Tarruell, M. Teichmann, J. McKeever, F. Chevy, and C. Salomon, Phys. Rev. Lett. **103**, 170402 (2009).  
[12] F. Chevy, Phys. Rev. A **74**, 063628 (2006).  
[13] C. Lobo, A. Recati, S. Giorgini, and S. Stringari, Phys. Rev. Lett. **97**, 200403 (2006),  
[14] R. Combescot, A. Recati, C. Lobo, and F. Chevy, Phys. Rev. Lett. **98**, 180402 (2007).  
[15] R. Combescot and S. Giraud, Phys. Rev. Lett. **101**, 050404 (2008),  
[16] N. Prokof’ev and B. Svistunov, Phys. Rev. B **77**, 020408 (2008).  
[17] M. W. Zwierlein, A. Schirotzek, C. H. Schunck, and W. Ketterle, Science **311**, 492 (2006).  
[18] G. B. Partridge, W. Li, R. I. Kamar, Y.-a. Liao, and R. G. Hulet, Science **311**, 503 (2006).  
[19] G. E. Astrakharchik and L. P. Pitaevskii, Phys. Rev. A **70**, 013608 (2004).  
[20] F. M. Cucchietti and E. Timmermans, Phys. Rev. Lett. **96**, 210401 (2006).  
[21] R. M. Kalas and D. Blume, Phys. Rev. A **73**, 043608 (2006).  
[22] M. Bruderer, W. Bao, and D. Jaksch, Eur. Phys. Lett. **82**, 30004 (2008).  
[23] S. Pilati and S. Giorgini, Phys. Rev. Lett. **100**, 030401

- (2008),
- [24] B.-B. Huang and S.-L. Wan, Chinese Physics Letters **26**, 080302 (2009).
- [25] J. Tempere, W. Casteels, M. K. Oberthaler, S. Knoop, E. Timmermans, and J. T. Devreese, Phys. Rev. B **80**, 184504 (2009).
- [26] M. Punk, P. T. Dumitrescu, and W. Zwerger, Phys. Rev. A **80**, 053605 (2009),
- [27] X. Cui and H. Zhai, Phys. Rev. A **81**, 041602 (2010).
- [28] S. Pilati, G. Bertaina, S. Giorgini, and M. Troyer, Phys. Rev. Lett. **105**, 030405 (2010),
- [29] P. Massignan and G. M. Bruun, Eur. Phys. J. D. **65**, 83 (2011).
- [30] R. Schmidt and T. Enss, Phys. Rev. A **83**, 063620 (2011).
- [31] J. M. Mathy, M. M. Parish, and D. A. Huse, Phys. Rev. Lett. **106**, 166404 (2011).
- [32] X.-W. Guan, Frontier of Physics **7**, 8 (2012).
- [33] W. Yi and X. Cui, Phys. Rev. A **92**, 013620 (2015),
- [34] R. Mao, X. W. Guan, and B. Wu, Phys. Rev. A **94**, 043645 (2016),
- [35] R. Schmidt, M. Knap, D. A. Ivanov, J.-S. You, M. Cetina, and E. Demler, arXiv:1702.08587 (2017).
- [36] M. Koschorreck, D. Pertot, E. Vogt, B. Fröhlich, M. Feld, and M. Köhl, Nature **485**, 619 (2012).
- [37] Y. Zhang, W. Ong, I. Arakelyan, and J. E. Thomas, Phys. Rev. Lett. **108**, 235302 (2012),
- [38] C. Kohstall, M. Zaccanti, M. Jag, A. Trenkwalder, P. Massignan, G. M. Bruun, F. Schreck, and R. Grimm, Nature **485**, 615 (2012).
- [39] M. Cetina, M. Jag, R. S. Lous, I. Fritsche, J. T. M. Walraven, R. Grimm, J. Levinsen, M. M. Parish, R. Schmidt, M. Knap, et al., Science **354**, 96 (2016).
- [40] F. Scazza, G. Valtolina, P. Massignan, A. Recati, A. Amico, A. Burchianti, C. Fort, M. Inguscio, M. Zaccanti, and G. Roati, Phys. Rev. Lett. **118**, 083602 (2017),
- [41] W. Casteels, T. Cauteren, J. Tempere, and J. T. Devreese, Laser Physics **21**, 1480 (2011).
- [42] W. Casteels, J. Tempere, and J. T. Devreese, Phys. Rev. A **86**, 043614 (2012).
- [43] S. P. Rath and R. Schmidt, Phys. Rev. A **88**, 053632 (2013).
- [44] B. Kain and H. Y. Ling, Phys. Rev. A **89**, 023612 (2014).
- [45] A. Shashi, F. Grusdt, D. A. Abanin, and E. Demler, Phys. Rev. A **89**, 053617 (2014).
- [46] W. Li and S. Das Sarma, Phys. Rev. A **90**, 013618 (2014).
- [47] F. Grusdt, Y. E. Shchadilova, A. N. Rubtsov, and E. Demler, Scientific Reports **5**, 12124 (2015).
- [48] L. A. P. n. Ardila and S. Giorgini, Phys. Rev. A **92**, 033612 (2015),
- [49] J. Vlietinck, W. Casteels, K. V. Houcke, J. Tempere, J. Ryckebusch, and J. T. Devreese, New Journal of Physics **17**, 033023 (2015).
- [50] Y. E. Shchadilova, F. Grusdt, A. N. Rubtsov, and E. Demler, Phys. Rev. A **93**, 043606 (2016),
- [51] R. S. Christensen, J. Levinsen, and G. M. Bruun, Phys. Rev. Lett. **115**, 160401 (2015).
- [52] J. Levinsen, M. M. Parish, and G. M. Bruun, Phys. Rev. Lett. **115**, 125302 (2015).
- [53] B. Kain and H. Y. Ling, Phys. Rev. A **94**, 013621 (2016),
- [54] R. Schmidt, H. R. Sadeghpour, and E. Demler, Phys. Rev. Lett. **116**, 105302 (2016),
- [55] Y. E. Shchadilova, R. Schmidt, F. Grusdt, and E. Demler, Phys. Rev. Lett. **117**, 113002 (2016),
- [56] F. Grusdt, R. Schmidt, Y. E. Shchadilova, and E. A. Demler, Phys. Rev. A **96**, 013607 (2017).
- [57] F. Grusdt, G. E. Astrakharchik, and E. A. Demler, arXiv:1704.02606 (2017).
- [58] M. Sun, H. Zhai, and X. Cui, Phys. Rev. Lett. **119**, 013401 (2017).
- [59] M. Sun and X. Cui, Phys. Rev. A **96**, 022707 (2017).
- [60] J. Catani, G. Lamporesi, D. Naik, M. Gring, M. Inguscio, F. Minardi, A. Kantian, and T. Giamarchi, Phys. Rev. A **85**, 023623 (2012).
- [61] M.-G. Hu, M. J. Van de Graaff, D. Kedar, J. P. Corson, E. A. Cornell, and D. S. Jin, Phys. Rev. Lett. **117**, 055301 (2016),
- [62] N. B. Jørgensen, L. Wacker, K. T. Skalmstang, M. M. Parish, J. Levinsen, R. S. Christensen, G. M. Bruun, and J. J. Arlt, Phys. Rev. Lett. **117**, 055302 (2016),
- [63] T. D. Lee, F. E. Low, and D. Pines, Phys. Rev. **90**, 297 (1953).
- [64] D. M. Edwards, Progress of Theoretical Physics Supplement **101**, 453 (1990).
- [65] H. Castella and X. Zotos, Phys. Rev. B **47**, 16186 (1993),
- [66] A. Lamacraft, Phys. Rev. B **79**, 241105 (2009),
- [67] C. J. M. Mathy, M. B. Zvonarev, and E. Demler, Nature Physics **8**, 881 (2012),
- [68] D. M. Edwards, Journal of Physics: Condensed Matter **25**, 425602 (2013),
- [69] F. Grusdt, N. Y. Yao, D. Abanin, M. Fleischhauer, and E. Demler, Nat. Commun. **7**, 11994 (2016),
- [70] J. B. McGuire, J. Math. Phys. **6**, 432 (1965),
- [71] J. B. McGuire, J. Math. Phys. **7**, 123 (1966),
- [72] E. Wigner and F. Seitz, Phys. Rev. **46**, 509 (1934),
- [73] L. Guan and S. Chen, Phys. Rev. Lett. **105**, 175301 (2010).
- [74] M. Olshanii, Phys. Rev. Lett. **81**, 938 (1998).
- [75] T. Bergeman, M. G. Moore, and M. Olshanii, Phys. Rev. Lett. **91**, 163201 (2003).
- [76] V. Peano, M. Thorwart, C. Mora, and R. Egger, New Journal of Physics **7**, 192 (2005),
- [77] X.-W. Guan, M. T. Batchelor, and C. Lee, Rev. Mod. Phys. **85**, 1633 (2013),
- [78] S. Giraud and R. Combescot, Phys. Rev. A **79**, 043615 (2009),
- [79] H. A. Bethe, Z. Phys. **71**, 205 (1931).
- [80] C. N. Yang, Phys. Rev. Lett. **19**, 1312 (1967),
- [81] M. Gaudin, Phys. Lett. A **24**, 55 (1967).
- [82] E. H. Lieb and F. Y. Wu, Phys. Rev. Lett. **20**, 1445 (1968),
- [83] E. Altman, E. Demler, and M. D. Lukin, Phys. Rev. A **70**, 013603 (2004).
- [84] S. Folling, F. Gerbier, A. Widera, O. Mandel, T. Gericke, and I. Bloch, Nature **434**, 481 (2005).
- [85] T. Rom, T. Best, D. van Oosten, U. Schneider, S. Folling, B. Paredes, and I. Bloch, Nature **444**, 733 (2006).
- [86] C. Chin, M. Bartenstein, A. Altmeyer, S. Riedl, S. Jochim, J. H. Denschlag, and R. Grimm, Science **305**, 1128 (2004).
- [87] J. Kinnunen, M. Rodriguez, and P. Törmä, Science **305**, 1131 (2004).
- [88] F. Grusdt and E. Demler, arXiv:1510.04934 (2015).